CHEMICAL ENGINEERING TRANSACTIONS
VOL. 66, 2018
A publication of AIDIC
The Italian Association of Chemical Engineering
Online at www.aidic.it/cet
Guest Editors: Songying Zhao, Yougang Sun, Ye Zhou

ISBN 978-88-95608-63-1; **ISSN** 2283-9216
DOI: 10.3303/CET1866114

Simulation of Active Disturbance Rejection Control for Cold-hot Water Mixer System

Jinquan Liao

Department of Internet of Things, Chongqing College of Electronic Engineering, Chongqing 401331, China
ChongqLiaojq@163.com

Motor overheating can cause the winding insulation, which will burn down the motor as it becomes serious. Dual channel of traditional PID control algorithm can reduce the motor temperature control accuracy and lead to motor overheating. In the simulation experiment, when the change of voltage and current remains under 30%, the improved algorithm can better realize accurate and stable temperature control than the traditional algorithm. The stability and accuracy increases by 36.5%, which suits for popularization and application.

1. Introduction

The control requirements on motor temperature has become increasingly demanding in industrial production. Besides, there are usually coupling relationships and time lag in all controlled parameters during the operation of motor. All parameters affect and restrict each other in the coupling relationship. In the time delay system, there is the time delay phenomenon in signal transmission (Wang et al., 2003; Yin et al., 2010). The coexistence of coupling relationship and time lag largely increases the difficulty in controlling each parameter during the operation of motor and it is difficult to control the motor temperature, resulting in the performance reduction. For this reason, the time-lag coupling relationship has become an important research direction in the field of motor running. Because of the extremely widespread applied range of motor temperature control methods, many experts lay importance on the motor temperature control methods, which have become the major research topic and have a large development space and practical value (Zheng et al., 2000; An et al., 2010; Han, 2009). With regard to controlling the motor temperature by using the traditional PID control algorithm, due to the great time lag and coupling in motor temperature, it is extremely difficult to describe it with any correct mathematical control model; thus, the precision in motor temperature control is reduced and the motor overheating can be caused (Chen and Xu, 2012).

2. Decoupling principles of traditional PID control

When the PID controller is used to regulate motor temperature, the temperature can be controlled by means of linear combination according to temperature change rate, integral time and derivative time. This can be expressed in Formula (1):

$$v(u) = L_Q(f(u) + \frac{1}{U_J}\int_0^u f(u)du + U_E\frac{df(u)}{du}) \quad (1)$$

In the formula, L_q signifies the motor temperature change rate; U_j signifies the integral time; *Ue* signifies the derivative time. The motor temperature control shall be expressed in formula (2):

$$\Delta v(l) = L_Q\Delta f(l) + L_J f(l) + L_E[\Delta f(l) - \Delta f(l-1)] \quad (2)$$

In the formula, L_q signifies the motor temperature change rate; $L_J=L_qU/U_J$ signifies the integral parameter; $L_E=L_qU_E/U$ signifies the differential parameter.

Please cite this article as: Liao J., 2018, Simulation of active disturbance rejection control for cold-hot water mixer system, Chemical Engineering Transactions, 66, 679-684 DOI:10.3303/CET1866114

3. Design of active disturbance rejection controller based on improved PID controller

3.1 Mathematical model of motor time-lag coupling system

To precisely control the motor temperature by using the active disturbance rejection controller, a transfer function on the temperature of motor time-lag coupling system is established by using the widely used step response curve method; this function can be expressed in Formula (3) below:

$$\begin{bmatrix} G_{11}(s) & G_{12}(s \\ G_{21}(s & G_{22}(s \end{bmatrix} = \begin{bmatrix} \dfrac{1.7e^{-30s}}{7s+1} & \dfrac{0.59e^{-27s}}{8s+1} \\ \dfrac{-0.6e^{-25s}}{10s+1} & \dfrac{1.5e^{-28s}}{9s+1} \end{bmatrix} \tag{3}$$

3.2 Structure of active disturbance rejection controller of motor temperature

The active disturbance rejection controller of motor temperature consists of three parts, the data tracker, the status viewer and the nonlinear feedback.

The data tracker has two functions: 1. It tracks the inputted parameters, processes input signal, makes the input data smooth, avoids overshoot and enhances the stability of system; 2.It provides the system with more reasonable differential signals and avoids the process of enlarging disturbance signals simultaneously in the process of signal generation with the traditional PID control method. In this paper, the data tracker is designed into a second-order discrete data tracker to meet the practical needs and is expressed in Formula (4) below:

$$\begin{cases} fh = fhan(x_1(k) - v(k), x_2(k), r, h_0) \\ x_1(k+1) = x_1(k) + h * x_2(k) \\ x_2(k+1) = x_2(k) + h * fh \end{cases} \tag{4}$$

In the formula, *fh* means the motor speed; *fhan* means the motor speed function; v signifies the input signal; x1 signifies the processed input signal; x2 signifies the first-order derivative of input signal; h signifies the step length; a shorter step length leads to lower noise while a longer step length will easily cause the system overshoot. h0 signifies the filter factor; when the h value remains the same and there is noise in the input signal, increasing h0 can lead to the generation of filtration; h, h0 and speed factor *r* are all parameters to be adjusted. Increasing the value of r can reduce the adjustment time and meanwhile increase the shock rate.

The status viewer is the key part of active disturbance rejection controller. Its inputs are the control parameter and system output parameter; its outputs are status variable and real-time action of system. The status viewer controls the internal and external disturbances as a whole and thus enhances the system's disturbance rejection property for internal and external disturbances. The following Formula (5) can be used to express the status viewer.

$$\begin{cases} e = z_1 - y \\ \dot{z}_1 = z_2 - \beta_1 e \\ \dot{z}_2 = z_3 - \beta_2 fal(e, 0.5, \delta) \\ \dot{z}_3 = -\beta_3 fal(1, 0.25, \delta) + bu \end{cases} \tag{5}$$

In the formula, z_1 and z_2 are the estimates of system input *y* and its first-order derivative. z3 is the new variable which disturbs the system; *fal* signifies the error change function. β1, β2, β3, δ b are adjustable parameters.

The input value in nonlinear feedback is the difference value of corresponding system status in the data tracker and status viewer and the real-time action of system acceleration in the status viewer. The numerical value in nonlinear feedback is the nonlinear function. The nonlinear feedback of third-order active disturbance rejection controller is expressed in Formula (6) below:

$$\begin{cases} e_1(k) = x_1(k) - z_1(k) \\ e_2(k) = x_2(k) - z_2(k) \\ u_0(k) = k_p fal(e_1(k), \alpha_1, \delta_1) + k_d fal(e_2(k), \alpha_2, \delta_2) \\ u(k) = u_0(k) - \dfrac{z_3(k)}{b_0} \end{cases} \tag{6}$$

In the formula, α1, α2, $\delta 1$, $\delta 2$, b0 are adjustable parameters while k_p, k_d are a proportionality coefficient and a differential coefficient respectively.

3.3 Decoupling principles of active disturbance rejection controller

Since the parameters influencing the motor temperature, such as voltage, frequency and all other variables, don't change with time, the active disturbance rejection controller designed in this paper shall be decoupled with the static decoupling method. In the motor temperature time-lag coupling system, under the condition of default power frequency, the main input parameters include current and voltage while the output parts include active power and heat. Therefore, the design of active disturbance rejection controller is two-input and two-output system and can be expressed in the Formula (7) below:

$$\begin{cases} \ddot{x}_1 = f_1(x_1, \dot{x}_1, x_2, \ddot{x}_2) + b_{11}u_1 + b_{12}u_2 \\ \ddot{x}_2 = f_2(x_1, \dot{x}_1, x_2, \ddot{x}_2) + b_{21}u_1 + b_{22}u_2 \\ y_1 = x_1, y_2 = x_2 \end{cases} \tag{7}$$

In the above formula, y_i is the output data of i channel; f_i(x1, ẋ1, x2, ẍ2) i=1, 2 is the "parameter of dynamic coupling"; b_{ij} is the amplification coefficient of input parameter and is also the function b_{ij}(x, ẋ, t) of status variable and time. In the matrix below,

$$B(x, \dot{x}, t) = \begin{bmatrix} b_{11}(x, \dot{x}, t) & b_{12}(x, \dot{x}, t) \\ b_{21}(x, \dot{x}, t) & b_{22}(x, \dot{x}, t) \end{bmatrix} \tag{8}$$

U=(x, ẋ, t)u signifies the "virtual parameter" and its relationship with channel i(i=1, 2) of system is described in Formula (9) below:

$$\begin{cases} \ddot{x}_i = f_i(x_1, \dot{x}_1, x_2, \dot{x}_2, t) + U_i \\ y_i = x_i \end{cases} \tag{9}$$

After the above-mentioned formula transformation, the following Formula (10) can be obtained:

$$\begin{cases} \ddot{x}_1 = f_1(x_1, \dot{x}_1, \cdots, x_m, \dot{x}_m) + U_1 \\ \ddot{x}_2 = f_2(x_2, \dot{x}_2, \cdots, x_m, \dot{x}_m) + U_2 \\ y_1 = x_1, y_2 = x_2 \end{cases} \tag{10}$$

The input parameter is decoupled in the above-mentioned formula. U_1 and U_2 can be used to respectively control the two channels. The motor temperature decoupling process is shown in figure below:

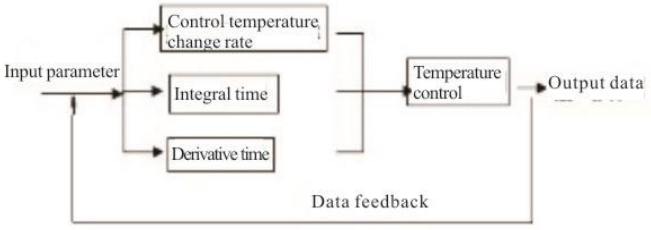

Figure 1: Schematic diagram for decoupling of active disturbance rejection controller of motor temperature

4. Simulation experiments

This paper carried out the simulation experiment on Matlab 7.0 platform. The experimental procedures are shown below:

1. Compile the control module of motor temperature active disturbance rejection controller with the S function;
2. Pack the independent modules in simulation; 3 Establish a simulation environment and take a simulation experiment on motor temperature.

4.1 Simulation of decoupling process

1. Parameter setting of active disturbance rejection controller:

The two channel values of active disturbance rejection controller are the same. If r=10000,h=0.001,β_{01}=0.001, β_{02}=0.001, β_{03}=0.01, h1=2.

2. Parameter setting of dual-channel PID controller:

If channel I: kp=0.05, ki=0.02 and kd=0 and channel II: kp=0.04, ki=0.03 and kd=0, the input amplitudes of channels I and II are the step signals of 1 and the simulation time is 600s.

According to the simulation experiment, the comparison results of the curve of active disturbance rejection control method and the curve of dual-channel control method are shown in the figure below:

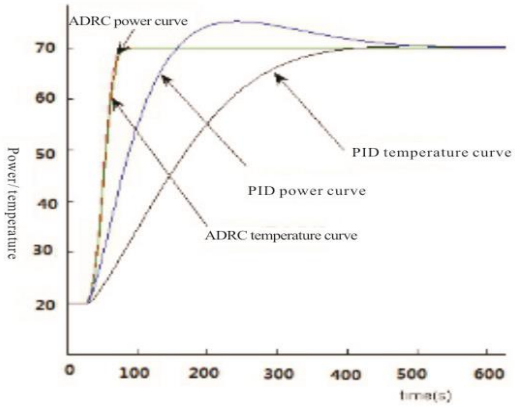

Figure 2: Comparison chart of dual-channel control curves

It can be seen from the comparison curves that the active disturbance rejection controller has a short response time, no overshoot, a favorable steady state; and the effects of the two channels are similar. The PID dual-channel controller has a long response time, has an overshoot phenomenon and a poor steady state, indicating that the active disturbance rejection controller has a better performance than the PID controller.

4.2 Research on robustness of the controlled object after time-lag change

As the motor current and voltage are not constant during motor startup, operation and brake, the time-lag coupling part of mathematical function of motor temperature also changes. Therefore, this paper specially takes an experiment on the time-lag change part of the controlled object during the simulation experiment.

During the simulation experiment, 30% of positive and negative changes in the numerical values of current in two channels of the controlled object were made and the voltage and the frequency data in the controller were kept unchanged to obtain the control curves, as shown in figures below:

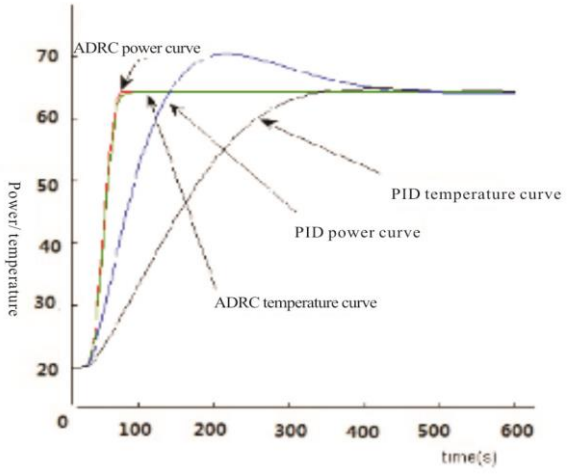

Figure 3: Curves of dual-channel responses with 30% increase in current

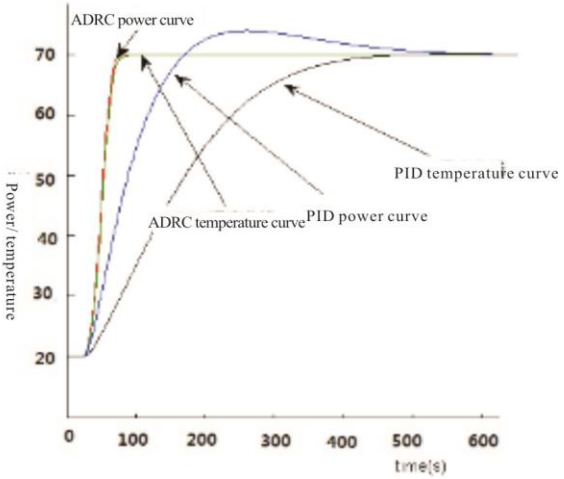

Figure 4: Curves of dual-channel responses with 30% decrease in current

It can be seen from the response curves that there are overshoot phenomena in both channels of PID and no overshoot phenomena in both channels of active disturbance rejection controller when there are 30% of positive and negative changes in current. It shows that the active disturbance rejection controller is superior to the PID controller regarding the dynamic response and stability.

The motor frequency and voltage etc. during operation are changeless on the premise of default power. If such numerical values change, the inertia coefficients in the mathematical model shall also change. For this reason, the designed active disturbance rejection controller must be able to adapt to the changes in inertia coefficients.

In the simulation laboratory, let there be 30% of positive and negative changes in voltage and frequency and keep the current unchanged to carry out a comparative experiment.

The control curves of dual-channel responses with 30% increases (decrease) in voltage and frequency are shown in the following figures:

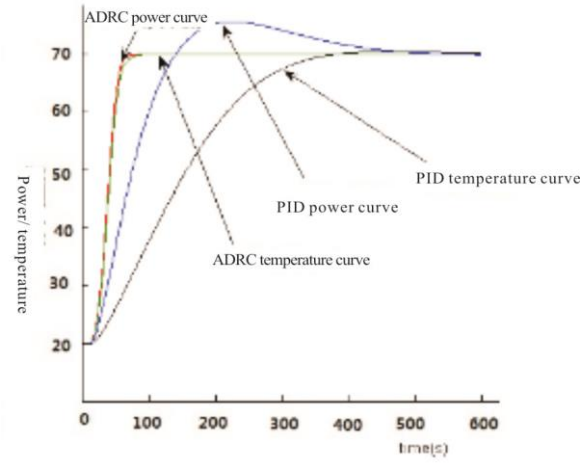

Figure 5: Curves of dual-channel responses with 30% increases in voltage and frequency

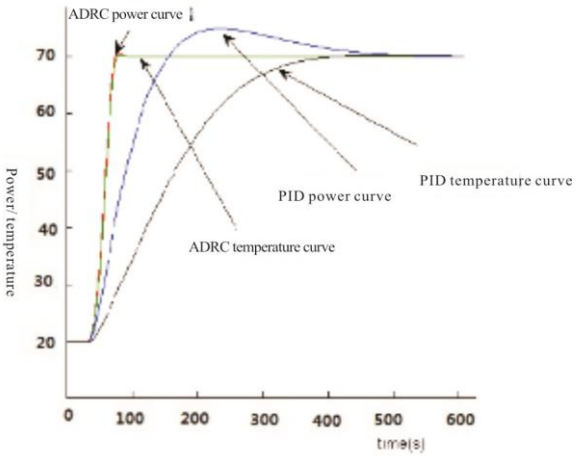

Figure 6: Curves of dual-channel responses with 30% decreases in voltage and frequency

It can be seen from the above response curves that both the dynamic and stable states of active disturbance rejection controller are better than those of the PID controller when there are changes in the voltage and frequency. Therefore, it shows that the active disturbance rejection controller can better adapt to the changes in inertia parameters.

5. Results and discussions

The real brushless DC motor is selected as the test object and the motor parameters are as follows: phase resistance: 3.234Ω; phase inductance: 11mH; rotational inertia: 0.0004 Kg m^2; rated speed: 2000r/min; number of pole-pairs: 6; damping coefficient: 0.003 N m s / rad.

Fig. 8 shows the curve collected from the brushless DC motor speed port. No-load startup is adopted; when it is 0.1s, abruptly add the load; the load torque is 3 N m. The three pictures in Fig. 9 respectively show the speed response curves with the traditional PID control, fuzzy PID control and PID control in this paper. From Fig. 8, it can be seen that the PID control method stated in this paper has a fast response speed and almost has no overshoot and steady state errors, indicating that this control method is better. From the partially enlarged Fig. 9, it can be clearly seen that, when the load is added abruptly, the PID control in this paper has a shorter adjusting time than the fuzzing PID; after the control process becomes stable, speed is always stable. This is consistent with the simulation results in the preceding statements, so there are significant advantages in the method proposed in this paper.

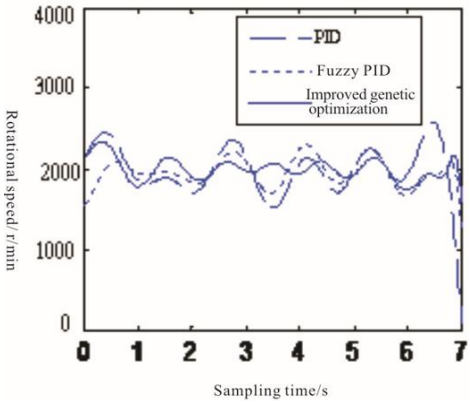

Figure 7: Statistics on sampling time and rotational speed

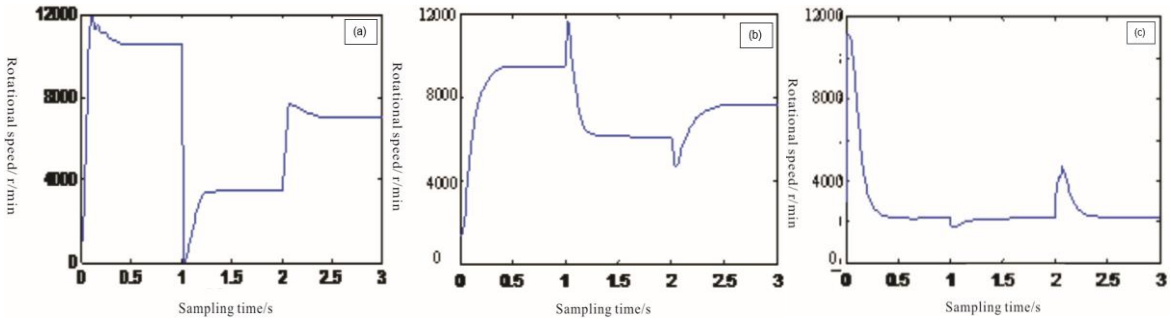

Figure 8: Speed simulation curve of brushless DC motor ((a) PID; (b) Fuzzy PID; (c) Improved method)

6. Conclusion

On the basis of traditional algorithms, this paper proposed a motor temperature control method based on the active disturbance rejection control and verified this algorithm of this paper through simulation experiments. As shown in the experimental results, the algorithm proposed in this paper has a faster response speed and almost has no overshoot and steady state errors, indicating that the control method in this paper is better and can be popularized, which is of great significance in motor temperature control in industrial production.

References

An J.Q., Wu M., Xiong Y.H., Wang C., 2010, Intelligent decoupling control method of furnace top pressure and its application, Information and Control, 39(2), 180-186.

Chen J.L., Xu N., 2012, Research and optimization of test methods for flow field temperature in a large-scale desulfurizer, Bulletin of Science and Technology, 12(28), 60-61, DOI: 10.3969/j.issn.1001-7119.2012.12.020.

Han J.Q., 2009, Active disturbance rejection control technology – control technology of uncertain factors of estimated compensation, Beijing: National Defence Industry Press.

Wang L., Wang X.X., Ma Y., 2003, Decentralized decoupling PID control over the neural network of IGA-based plate shape and thickness, Computer simulation, 20(12), 82-85.

Yin X.L., Zheng E.R., Zhang L., 2010, Improved fuzzy immune PID control over quantitative moisture during papermaking process, Computer Measurement and Control, 18(2), 354-356.

Zheng E.R., Zhang L., Yang J.Q., 2000, Neural network PID and its application in quantitative moisture control of paper sheet, Basic Automation, 7(3), 198-201, DOI: 10.3969/j.issn.1671-7848.2000.03.003.